Initial Results of UCLA SETI Observations

Jean-Luc Margot[a,b], Adam Greenberg[b], Akshay Shinde[c], Yashaswi Alladi[c], Srinivas Prasad MN[d], Oliver Bowman[a], Callum Fisher[b], Szilard Gyalay[b], William McKibbin[b], Brittany Miles[b], Donald Nguyen[b], Conor Power[d], Namrata Ramani[e], Rashmi Raviprasad[b], Jesse Santana[b]

[a] *Department of Earth, Planetary, and Space Sciences, University of California, Los Angeles, jlm@epss.ucla.edu*
[b] *Department of Physics and Astronomy, University of California, Los Angeles*
[c] *Department of Computer Science, University of California, Los Angeles*
[d] *Department of Electrical Engineering, University of California, Los Angeles*
[e] *Department of Materials Science and Engineering, University of California, Los Angeles*

Abstract

We describe our search for signals of an artificial nature in our observations of exoplanets with the 100 m diameter Green Bank Telescope (GBT). Observations took place on April 15, 2016 and focused on 14 host stars associated with exoplanets discovered as part of NASA's Kepler Mission. We recorded the in-phase and quadrature voltage samples of the baseband signals corresponding to two linear polarizations. The center frequency was 1500 MHz and the bandwidth was 800 MHz. Each source was observed twice for 2.5 minutes in an ON-OFF sequence, yielding a total integration time of 5 minutes per source. In our initial analysis, we obtained 126 power spectra of a subset of each one of the 28 scans at a frequency resolution of ~3 Hz. We shifted and summed the powers to examine 255 Doppler drift rates covering ±9 Hz/s in linearly spaced increments of 0.07 Hz/s. Any signal with a non-zero Doppler drift rate and signal-to-noise ratio (SNR) in excess of 10 was flagged as a candidate, yielding ~half a million candidate signals whose characteristics were recorded in a structured query language (SQL) database. We examined the 10 signals with highest SNR in each 3.125 MHz band, resulting in ~10,000 narrowband candidate signals. Candidate signals that were associated with more than one source on the sky were classified as human-generated radio-frequency interference (RFI). We also eliminated candidate signals that did not appear in both scans of the same source. All 66 of the remaining candidate signals were scrutinized and none could be attributed to an extraterrestrial source. Additional analysis of the full duration of each scan is ongoing.

Keywords: SETI, Kepler, exoplanets, habitable, radio, GBT

1. Introduction

Analysis of Kepler Mission data suggests that the Milky Way Galaxy includes billions of Earth-like planets in the habitable zone of their host star [e.g., 1]. The possibility that intelligent and communicative life forms developed on one or more of these worlds behooves us to conduct a search for extraterrestrial intelligence. Here we describe an L-band radio survey of 14 exoplanets selected from the Kepler Mission field, most of which are ranked at the top of a habitability scale [2]. Our analysis methods are generally similar to those used by Siemion et al. [3], but our survey samples a different slice of the search volume. Sections 2, 3, 4, 5 describe the observations, analysis, results, and conclusions, respectively.

2. Observations

We selected 14 exoplanet host stars from the Kepler Catalog (Table 1). A majority of these stars host small ($R_p < 2 R_E$) planets in the habitable zone (HZ) [2]. Our observing sequence was based on a solution to the traveling salesman problem in order to minimize the time spent repositioning the telescope. Each target was observed twice in the following 4-scan sequence: target 1, target 2, target 1, target 2. The integration time for each scan was 150 s, which was calculated by dividing the observing time remaining after our calibration procedures by 28 and subtracting the expected average overhead time.

Table 1. Observing sequence

Host star	**Analyst**	**Notes ***
Kepler-399	Yashaswi	
Kepler-186	Brittany	Cat. 1
Kepler-452	Akshay	Cat. 2
Kepler-141	Rashmi	
Kepler-283	William	Cat. 1
Kepler-22	Srinivas	Cat. 4
Kepler-296	Namrata	Cat. 1
Kepler-407	Szilard	
Kepler-174	Jesse	Cat. 2
Kepler-62	Adam	Cat. 1
Kepler-439	Donald	
Kepler-438	Callum	
Kepler-440	Jean-Luc	Cat. 2
Kepler-442	Conor	Cat. 1

* Categories 1/3 and 2/4 refer to the conservative and optimistic HZ of Kane et al. [2], respectively. In multi-planet systems, only the lowest category is listed.

We conducted our observations with the GBT [4] on April 15, 2016, 16:00-18:00 Universal Time (UT). We recorded both linear polarizations of the L-band receiver, which has a frequency range of 1.15–1.73 GHz. Over this frequency range, the full-width half maximum (FWHM) beam width of the telescope is 11–7.3 arcmin. The aperture efficiency is ~72% and the telescope gain is ~2 K/Jy. Typical system temperatures are ~20 K. The L-band receiver is located at the Gregorian focus of the telescope, which was designed with an off-axis reflector to minimize stray radiation.

We used the GUPPI backend [5] in baseband recording mode and sampled 800 MHz of bandwidth from 1.1 to 1.9 GHz, of which ~600 MHz are useful. The signal was channelized into 256 channels of 3.125 MHz bandwidth each. The raw voltages of the in-phase and quadrature channels were sampled at 8-bit quantization, but only the most significant 2 bits were retained and packed into words by on-board field programmable gate arrays (FPGAs). Eight computers handled the transfer of the data to 8 disk arrays at an aggregate rate of 800 MB/s or 2.88 TB/h.

Calibration procedures at the beginning of our observing window consisted of recording a monochromatic tone at 1501 MHz (center frequency + 1 MHz), performing a peak and focus procedure on a bright radio source near the Kepler field, and observing a bright pulsar near the Kepler field (PSR B2021+51) [6].

3. Analysis

3.1 Validations

We verified the validity of our data-processing pipeline by analyzing the monochromatic tone data and recovering the signal at the expected frequency. We also folded the pulsar data at the known pulsar period and recovered the characteristic pulse profile (Fig. 1).

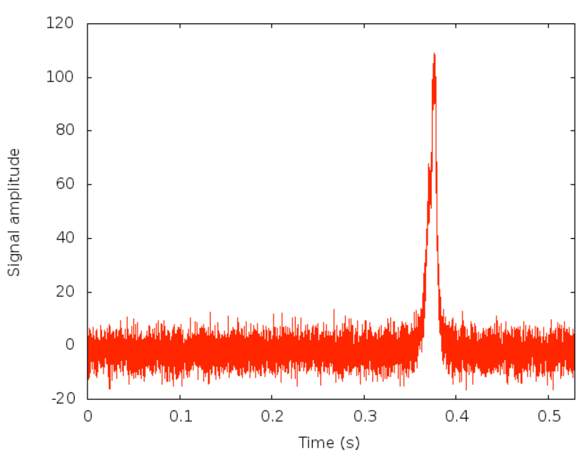

Fig. 1. Detection of PSR B2021+51 with the GBT.

3.2 Spectral analysis

We unpacked the data to 4-byte floating point values, computed Fourier transforms of the complex samples with the FFTW routine [7], and calculated the signal power at each frequency bin. We used a Fourier transform length of 2^{20}, which yielded a frequency resolution of 2.98 Hz. We stored 126 consecutive power spectra, corresponding to 42 s of each scan, in frequency-time arrays of 2^{20} columns and 126 rows. The average noise power was subtracted and the array values were scaled to the standard deviation of the noise power.

3.2 Drift rate analysis

Because a signal emitted by an extraterrestrial source experiences a time-variable Doppler shift due to the rotational and orbital motions of Earth and the unknown motion of the emitter, we examined a range of Doppler drift rates. We implemented a tree algorithm [8,3] to investigate 255 Doppler drift rates covering ±8.88 Hz/s in linearly spaced increments of 0.0694 Hz/s. This algorithm reads the time-frequency arrays and sums all the powers corresponding to each one of 128 possible drift rate values. Its application resulted in two frequency-drift rate arrays of 2^{20} columns and 128 rows for each scan, one for positive Doppler drift rates and one for negative Doppler drift rates.

3.4 Candidate signal detection

Signals with SNR larger than 10 were stored in a SQL database for additional analysis. Each candidate signal was assigned a unique identifier in the database. A signal from a source at rest or in uniform motion with respect to the observer exhibits no drift in the value of the Doppler shift. Signals from extraterrestrial sources, unless cleverly compensated for a specific location on Earth, experience a Doppler drift due to the rotational and orbital motions of both the Earth and the emitter. For these reasons, we flagged all signals with a zero Doppler drift rate as likely terrestrial and eliminated them from further consideration.

3.5 Rejection algorithms

To further distinguish between RFI and genuine extraterrestrial signals, we implemented two additional filters. First, we flagged any signal that was not detected in both scans of the same source. This filter can rule out many signals from terrestrial emitters that temporarily enter the beam (e.g., satellites). Second, we flagged any signal that was detected in more than one position on the sky. This filter can rule out many terrestrial signals that are detectable through the antenna sidelobes. A logical AND was used to automatically flag candidate signals that remained for consideration after the rejection steps.

Our rejection filters used the scan times, durations, frequencies, Doppler drift rates, and frequency resolutions stored in the SQL database to properly recognize signals from the same emitter observed at different times.

3.6 Evaluation of remaining candidates

Signals that remained for consideration were easily recognized by the value of the relevant database flag. A display program was invoked to automatically produce a frequency-time diagram of the remaining candidates. Examination of the plots revealed groups of signals that can be attributed to the same source of RFI. In some cases, our rejection filter logic failed because the Doppler behavior was erratic.

3.7 Future work

A number of improvements are planned to our existing data processing pipeline (Fig. 2), including more robust rejection filters and better flags for RFI classification.

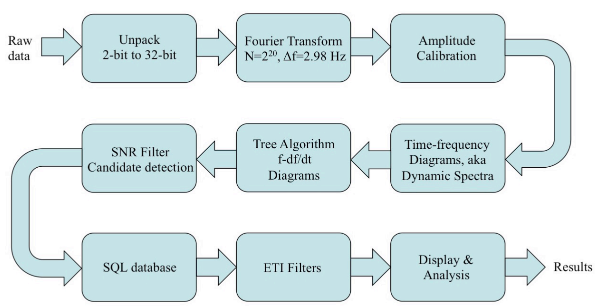

Fig. 2. Schematic of the data processing pipeline

4. Results and Discussion

We detected over a million signals with SNR>10. About half of these candidates have zero Doppler drift rates, which we flagged and eliminated from further consideration. To keep the search manageable, we selected 10 signals with the highest SNR in each 3.125 MHz wide frequency band, which yielded 10185 candidate signals. Our rejection filters (Section 3.5) eliminated 99.35% of these candidates. A total of 66 candidate signals remained. Upon closer inspection, all of the remaining signals were ruled out either because they were attributable to a known interferer (e.g., GPS, GLONASS) or because they appeared in more than one direction on the sky, suggesting sidelobe contamination. One such signal shows clear evidence of intelligence (Fig. 3), shifting by ± ~10 Hz as a function of time in a manner similar to that used in the 1974 Arecibo message [9]. Even though we focused on narrowband signals, broadband signals are sometimes detected by our current pipeline, whether or not they are flanked by a narrowband side carrier (Fig. 4).

Although no extraterrestrial signals have been identified to date, it is important to recall that our study encompassed a minuscule fraction of the search volume. The fraction of the sky that was covered in our search is 14 times the solid angle of the GBT beam. At the lowest frequency of our search, each beam corresponds to less than a millionth of the sky area. Considering all 14 sources, we covered about 1 part in 100,000 of the entire sky. Our observations lasted a total of 5 minutes on each source, which is 1 part in 100,000 of a terrestrial year. Our useful bandwidth spanned ~600 MHz, which is a small fraction of the electromagnetic spectrum available for telecommunications.

5. Conclusions

We described the results of a search for narrowband signals from extraterrestrial sources using 2 hours of GBT telescope time. In our initial processing of the data, none of the signals could be attributed to an extraterrestrial source. Additional analysis is warranted.

Our observations were designed, obtained, and analyzed by students enrolled in a UCLA course titled "Search for Extraterrestrial Intelligence: Theory and Applications". SETI observations provide a superb educational opportunity for students in astrophysics, computer science, engineering, mathematics, planetary science, and statistics. In this work, 5 graduate students and 9 undergraduate students at UCLA learned valuable skills related to radio astronomy, telecommunications, programming, signal processing, and statistical analysis. A syllabus and a detailed narrative of the course are available at http://seti.ucla.edu.

Acknowledgements

We thank Janet Marott and Larry Lesyna for the financial support that made this work possible.

We are grateful to Ryan Lynch, Frank Ghigo, Ron Maddalena, and Wolfgang Baudler for assistance with the GBT observations. We are grateful to the designers and funders of GUPPI for making the system available to us, with special thanks to John Ford and Paul Demorest.

References

[1] W. J. Borucki, KEPLER Mission: development and overview, Reports on Progress in Physics 79 (3) (2016) 036901. doi:10.1088/0034-4885/79/3/036901.

[2] S. R. Kane, M. L. Hill, J. F. Kasting, R. K. Kopparapu, E. V. Quintana, T. Barclay, N. M. Batalha, W. J. Borucki, D. R. Ciardi, N. Haghighipour, N. R. Hinkel, L. Kaltenegger, F. Selsis, G. Torres, A Catalog of Kepler Habitable Zone Exoplanet Candidates, ArXiv e-prints 1608.00620.

[3] A. P. V. Siemion, P. Demorest, E. Korpela, R. J. Maddalena, D. Werthimer, J. Cobb, A. W. Howard, G. Langston, M. Lebofsky, G. W. Marcy, J. Tarter,

A 1.1–1.9 GHz SETI Survey of the Kepler Field. I. A Search for Narrow-band Emission from Select Targets, ApJ 767 (2013) 94. doi:10.1088/0004-637X/767/1/94.
[4] P. R. Jewell, R. M. Prestage, The Green Bank Telescope, in: J. M. Oschmann, Jr. (Ed.), Ground-based Telescopes, Vol. 5489 of Proc. SPIE, 2004, pp. 312–323. doi:10.1117/12.550631.
[5] S. M. Ransom, P. Demorest, J. Ford, R. McCullough, J. Ray, R. DuPlain, P. Brandt, GUPPI: Green Bank Ultimate Pulsar Processing Instrument, in: American Astronomical Society Meeting Abstracts #214, Vol. 214 of American Astronomical Society Meeting Abstracts, 2009, p. 605.08.
[6] R. N. Manchester, G. B. Hobbs, A. Teoh, M. Hobbs, The Australia Telescope National Facility Pulsar Catalogue, AJ 129 (2005) 1993–2006. doi:10.1086/428488.
[7] M. Frigo, S. G. Johnson, The design and implementation of FFTW3, Proceedings of the IEEE 93 (2) (2005) 216–231, special issue on “Program Generation, Optimization, and Platform Adaptation".
[8] J. H. Taylor, A Sensitive Method for Detecting Dispersed Radio Emission, A&AS 15 (1974) 367.
[9] The staff at the National Astronomy and Ionosphere Center, The Arecibo message of November, 1974, Icarus 26 (1975) 462–466. doi:10.1016/0019-1035(75)90116-5.

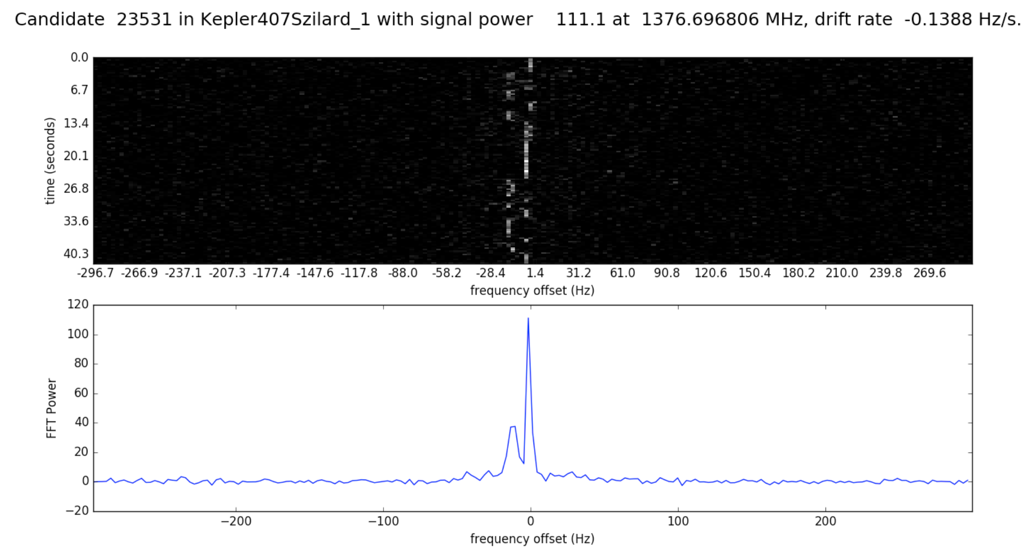

Fig. 3. Candidate signal attributed to terrestrial RFI

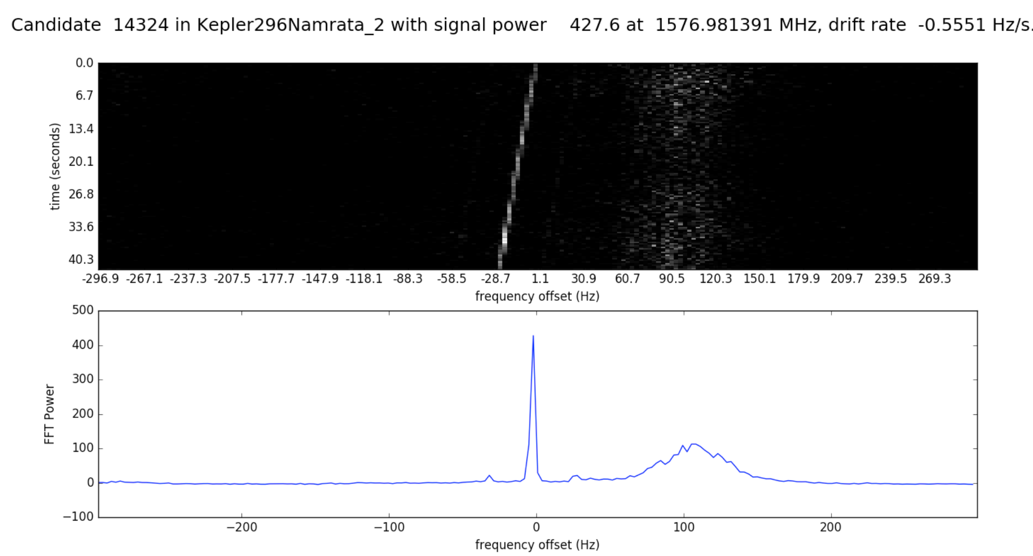

Fig. 4. Candidate signal attributed to terrestrial RFI